Index 351660
ISSN 0004-0746

POLISH ACADEMY OF SCIENCES
Electrical Engineering Committee

ARCHIVES OF ELECTRICAL ENGINEERING

VOL. 60 (237) · 3/2011

QUARTERLY JOURNAL

Poznań 2011

ARCHIVES OF ELECTRICAL ENGINEERING VOL. 60(3), pp. 371-380 (2011)

DOI 10.2478/v10171-011-0032-5

A study on permanent magnet topologies for hybrid bearings for medical drives applied in Ventricular Assist Devices

ANDRÉ POHLMANN, KAY HAMEYER

Institute of Electrical Machines, RWTH Aachen University
Schinkelstrasse 4, D-52056 Aachen, Germany
e-mail: Andre.Pohlmann@iem.rwth-aachen.de

(Received: 02.07.2010, revised: 08.08.2011)

Abstract: In industrialized countries cardiovascular diseases are the major cause of death. The last clinical therapy option for some patients, suffering from terminal heart diseases, is donor heart transplantation. As the available number of donor organs is decreasing, many patients die while waiting for a transplant. For this reason Ventricular Assist Devices (VADs), which can mechanically support the human heart to achieve a sufficient perfusion of the body, are under development. For an implantable VAD, design constraints have to be deduced from the physiological conditions in the human body. In case of a VAD drive, these constraints are for example dimensions, electric losses, which might result in an overheating of blood, and a long durability. Therefore a hybrid permanent magnet hydrodynamic bearing is designed in this paper, which works passively and contactless. Based on Finite Element simulations of magnetic fields, various permanent magnet topologies are studied in terms of axial forces and stiffness.

Key words: Ventricular Assist Device, VAD, Finite Element Method, FEM, magnetic bearings

1. Introduction

According to the World Health Organization, cardiovascular diseases are the major cause of death in industrialized countries [1]. In the final stage of heart failure, a donor heart transplantation is the last clinical therapy option. While the number of available donor hearts is decreasing, the demand for them is rising worldwide [2, 6].

Therefore, Artificial Hearts (AHs) are developed as a supporting therapy alternative. In general AHs can be distinguished between Total Artificial Hearts (TAHs) and Ventricular Assist Devices (VADs). A TAH serves as a human heart replacement and should sustain the life of patients until a donor organ is available. In science a main objective is to enhance its operation durability with the future prospect that the TAH can replace the human heart for the patients' lifetime. If the patients' heart retains some perfusion capabilities, a VAD can be im-

planted to support the human heart to generate a sufficient perfusion of the body. In such a case there are two possible therapy strategies. The first one bridges the time until a transplant is available, similar to the TAH, while the second one bridges the time until the heart has recovered. A recovery might be possible due to the unloading of the weak human heart.

As an example of a left Ventricular Assist Device (LVAD) system the Heartmate II is shown in Figure 1, which is approved by the United States Food and Drug Administration (FDA) since 2008. The implanted pump unit generates a continuous blood flow and has blood immersed and conventional bearings [3, 5]. It is connected between the left ventricle of the human heart and the ascending aorta. The pump unit is supplied and controlled by external batteries and controller via an electric driveline penetrating the skin. This design has two major drawbacks, which are both limiting the durability of this VAD. First, the driveline is a source of infections.

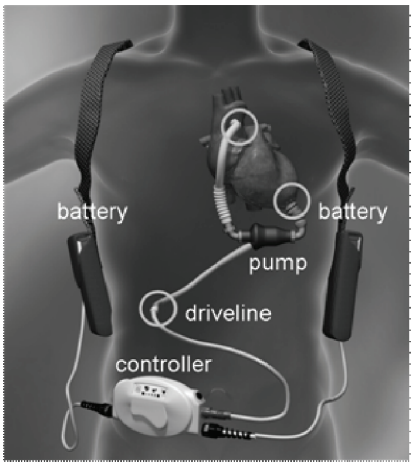

Fig. 1. Schematic of the VAD system Heartmate 2

This problem can be solved by applying a so called transcutaneous energy transmission systems (TET-systems), which have been described earlier e.g. by H. Miura et. al. [4]. Second, the applied bearings are conventional and therefore wear prone. Therefore, this contribution focuses on study of permanent magnet topologies for a hybrid hydrodynamic permanent magnet bearing. Such an assembly comprises the advantages of a passive and contactless bearing.

VAD design

During Heart Assist operation the most important objectives are obviously a sufficient perfusion of the human body without blood and/or tissue damage. In general the requirements for the quality of a LVAD are higher than those of a right Ventricular Assist Device (RVAD). The reason is the higher mean pressure of the systemic blood circuit (100 mmHg) when compared to the pulmonary blood circuit (18 mmHg). This specification requires higher forces or torque to generate the sufficient perfusion with the drive system. This reflects on the constraints for the drive design, including its bearings. In medicine the important causes for blood damage are hemolysis, thrombogenicity or denaturation. High shear forces, stagnation of the

blood, not biocompatible material and coarse surfaces are the main factors yielding hemolysis and thrombogenicity. These effects have to be minimized in the design of the pump unit, based on the shape of the flow guiding, the shape of the impeller and/or its operation speed. The risk of hemolysis can be reduced by applying contactless bearings. In the human body denaturation starts at body temperature of 40˚C and is irreversible for temperatures above 42˚C. Denaturation yields a deformation of the biomolecular structure of the proteins in the blood causing its destruction. Therefore an overheating of the blood, caused by the losses of the active VAD components, has to be minimized.

Figure 2 represents the scheme of a radial flow LVAD. It has an axial inlet. The blood flow is diverted into the radial direction by the impeller. The impeller is attached to the rotor, which in combination with the stator, forms the drive of the LVAD. In this design the bearing is realized with a hydrodynamic bearing. In general hydrodynamic bearings rely on a thin film of blood and are classified as contactless and passive. Its repelling forces depend on its geometry, which is determined during the hydraulic design process. This VAD is operated by a Brushless DC (BLDC) disc type motor (Fig. 3). In order to achieve a high efficiency a field oriented control with block shaped currents is applied. This allows for a sensor less control.

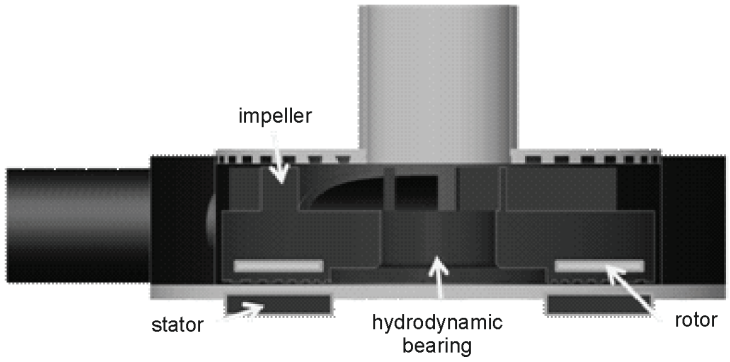

Fig. 2. Scheme of a Left Ventricular Assist Device

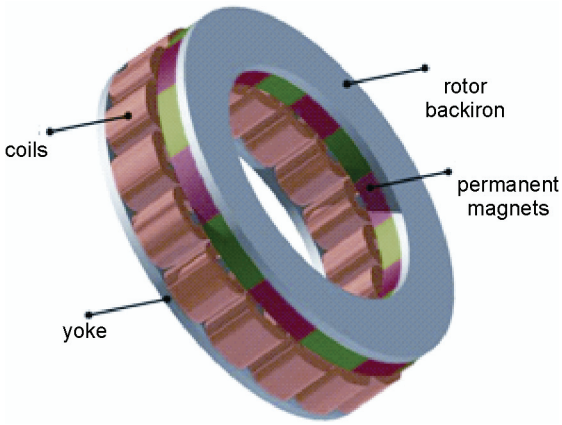

Fig. 3. CAD drawing of a VAD drive

The rotor consists of a ferromagnetic steel ring, which houses 16 axially magnetized, neodymium iron boron magnets (NdFeB) with a remanent induction of 1.4 T at 20°C. There are 18 coils, made of a rectangular shaped copper wire in three phase star connection, attached to the ferromagnetic stator yoke. The copper fill factor amounts to approx. 60%. In the desired operation point the air gap is 1 mm. Table 1 collects the design parameters of the introduced drive, which are its output torque of 12 mNm, a speed of 2500 rpm and its maximum outer dimensions including the air gap between stator and rotor, allowing for a perfusion of 6l. of blood per minute against an mean aortic pressure of 100 mm Hg.

Table 1. Design parameters

Design objectives	
nominal speed	2500 rpm
nominal torque	12 mNm
drive height	10 mm
outer radius	< 20 mm

2. Study of permanent magnet topologies

In the initial design of the presented drive the coils were partially filled with ferromagnetic steel and air and the resulting axial forces were compensated by a hydrodynamic bearing, relying on a thin layer of blood without friction. In a next step the efficiency of the drive should be increased. As the output power of an electrical motor is directly linked to its torque generation, an increased torque generation also improves the drive's efficiency. Basically the torque generation can be calculated by the cross product of the rotor radius r and the radial force F_{rad}.

$$\vec{T} = \vec{r} \times \vec{F}_{\mathrm{rad}}\,. \tag{1}$$

The radial force is given by the following Equation 2:

$$\vec{F}_{\mathrm{rad}} = I \cdot (\vec{l} \times \vec{B}) \cdot \vec{e}_{\mathrm{rad}}\,. \tag{2}$$

In this geometry the active coil length l is only dependent on the drive geometry and is therefore assumed to be constant. If the coil supply current I is kept constant, the radial force as well as the drives efficiency can be maximized by increasing the magnetic induction B. This is achieved by completely filling the stator teeth with ferromagnetic material with a relative permeability μ_r (~1000) that is higher than the μ_r of air (ca. 1). Additionally stray flux is reduced by this arrangement yielding a higher efficiency. But according to Equation 3,

$$\vec{F}_{\mathrm{axial}} = \frac{B^2 \cdot A}{2 \cdot \mu_0} \cdot \vec{e}_{\mathrm{axial}}\,, \tag{3}$$

this design increases the axial forces F_{axial} as well, when compared to the previous topology, which can not be compensated by the hydrodynamic bearing. In Equation 3 A is the surface

area penetrated by the magnetic induction B, which is given by the drive geometry. The constant vacuum permeability is given by the variable μ_0. As there is available space in the motor, the idea is to support it with permanent magnet material, to keep the advantages of passive and contactless bearings. According to Earnshaw's law [7],

$$2 \cdot k_\rho + k_z \leq 0, \tag{4}$$

permanent magnets are always instable in one direction. This can be explained by the sum of the axial k_z and radial stiffness k_ρ, which is always lower than zero. For this reason the repelling permanent magnets should compensate the axial attracting forces of the drive, while the hydrodynamic bearing is stabilizing the drive in radial direction and provides additional stabilization capabilities for the axial direction.

For the evaluation of the investigated permanent magnet topologies the maximum available space in the drive, limited by the inner and outer radius r_i and r_o respectively and the height of the stator h_s and rotor h_r, is used to generate the maximum possible magnetic field. Table 2 collects the dimensions of the presented topologies (Figs. 4, 5), which are both axially magnetized.

Table 2. Dimensions of the permanent magnets topologies

Parameter	[mm]
Stator height	6 mm
Rotor height	3 mm
Air gap	0.75 ~ 1.2 mm
Inner radius r_i	5.5 mm
Outer radius r_o	10 mm
Medium radius r_m	7.6 mm

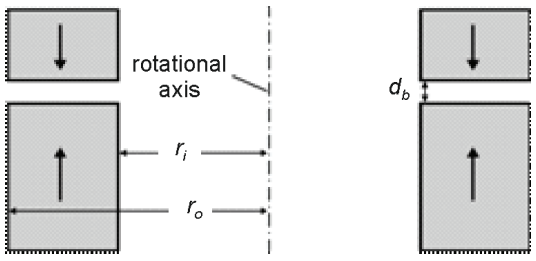

Fig. 4. Non segmented axial magnetized permanent magnet

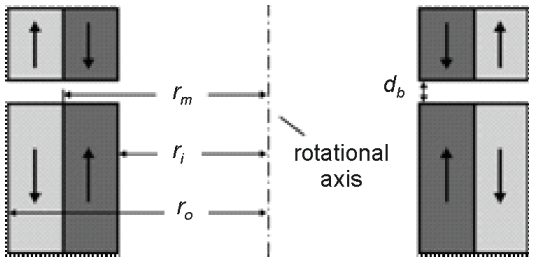

Fig. 5. Double segmented axial magnetized permanent magnet

The second topology is divided into two segments, which are magnetized in directions that are reverse to each other. By varying the medium radius r_m of this topology, the geometry yielding the maximum possible force output is determined. For the evaluation and comparison of both topologies static and three dimensional magnetic Finite Element (FE) simulations were performed. As the remanent magnetic induction is dependent on the material temperature, it has been adjusted for the simulation by applying Equation 5. It amounts to 1.37 T at an assumed surrounding tissue temperature of 40 °C and a temperature coefficient α of −12%/°K and a remanent induction $B_{r,20}$ of 1.4 T at room temperature.

$$B_r = B_{r,20}\left(1+\alpha\left(T-T_{20}\right)\right). \tag{5}$$

In Figure 6 the resulting simulated forces of the two arrangements are presented for air gaps in the range of 0.75 and 1.2 mm. At an air gap of 1 mm there is an intersection between them. For larger air gaps the non segmented permanent magnet topology yields higher repelling forces.

Additionally the axial stiffness of the topologies, describing the variation of axial forces F in dependency of the air gap z, have been determined by the analytical calculation of the differential quotient of the forces acting at neighbored air gap thicknesses d_{bx} and d_{bx+1}.

$$k_z = \frac{\Delta F}{\Delta z} = \frac{F(d_{bx}) - F(d_{bx+1})}{d_{bx+1} - d_{bx}}. \tag{6}$$

As the air gap d_b in the drive should have a maximum width of 1 mm, the double segmented permanent magnet bearing can generates higher forces and stiffness (see Figs. 6, 7) when compared to the non segmented alternative. This variant is therefore more promising for a stable motor and VAD operation.

When comparing the non and double segmented topologies, the stray flux is reduced due to a reduction of the magnetic short circuits. Although a further segmentation or additional flux guiding iron parts might improve the results further, these options are not considered here due to manufacturing reasons. When changing from axial to radial magnetization, the resulting maximum forces for the non – and double segmented topology amount to 48 and 55 N respectively. Additionally the resulting stiffness is lower for the radial magnetized variant. For this reason the double segmented and axial magnetized permanent topology is applied as an bearing for the following drive modifications.

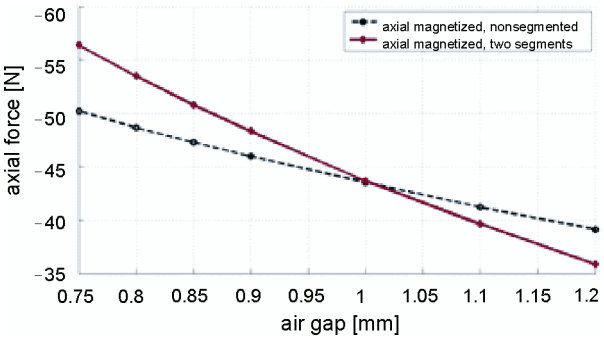

Fig. 6. Force vs. air gap of magnetic bearings

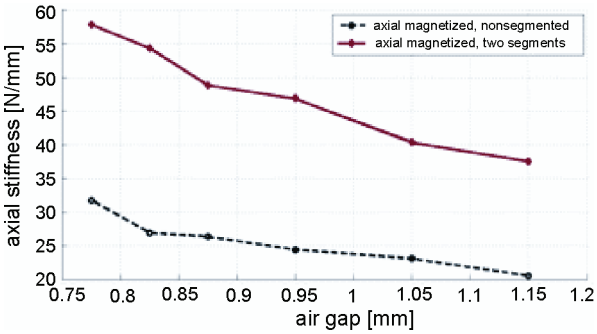

Fig. 7. Stiffness vs. air gap of magnetic bearings

3. Evaluation of the drive design

The next step contains the determination of the axial force and stiffness of the introduced drive design, which are position dependent due to the occurrence of reluctance forces. As the drive assembly is symmetric, an evaluation of a drive rotation of 120°el is sufficient. Due to the inertia of the rotor and its nominal rotational speed of 2500 rpm, the axial force and stiffness are calculated by determining the mean value of the position dependent force and stiffness. The stator yoke as well as the rotor back iron is made of solid ferromagnetic steel (9S20) with a saturation induction of 1.7 T. According to Figure 8 the rotor backiron is saturated.

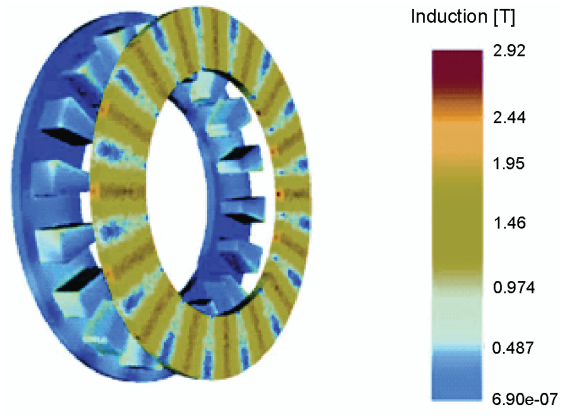

Fig. 8. Distribution of the induction inside the BLDC drive

Additionally high stray flux occurs due to the relatively high air gap. For these reasons a quasi transient, three dimensional and non-linear solver is applied for the Finite Element (FE) simulation of the magnetic induction and the resulting forces. When comparing the axial forces of the current drive design with 16 magnetic poles (see Fig. 9) and of the double segmented permanent magnet bearing, a stable VAD operation is not possible without decreasing the attracting forces in the drive.

According to Equation 3 the magnetic induction B or the surface area A, penetrated by the magnetic induction, has to be reduced. For the first option two possibilities have been considered. One option is to decrease the number of poles and therefore the number of permanent magnets in the rotor. This yields a more homogeneous air gap field and a reduced attraction force, a lower axial stiffness and torque. Due to the higher relative permeability of ferromagnetic iron, the magnetic induction inside the iron is higher than in air. For this reason the axial force can also be reduced by decreasing the stator teeth height, yielding coils partially filled with air and iron. This option, as well as a reduction of the surface area A, requires significant modifications in the drive design. The simpler way is to reduce the number of poles by adjusting the axial magnetization direction of neighbored rotor permanent magnets. In Figure 8 the axial force of a drive with 16 and 8 poles are presented. The 8 pole variant generates lower forces for air gaps in the range of 0.75 and 1 mm. This is the desired operation range of the drive. Outside the 1 mm air gap range, this variant yields a higher axial force due to its flatter force vs. displacement characteristic.

In Figure 10 the absolute attracting and repelling axial forces of the drive and the applied permanent magnet bearing respectively are presented. For air gaps d_B between 0.75 and 1.2 mm the attractive forces exceed the repelling forces by approx. 5N, while the slope of both graphs is in the same range. Therefore the design of the drive and bearings is modified according to Figure 11. By operating the drive with different air gaps between stator and rotor and upper and lower bearing, the force characteristic of the bearing is shifted as shown in Figure 10.

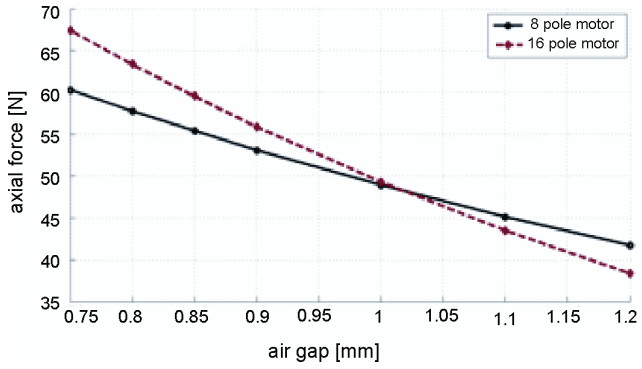

Fig. 9. Axial forces in BLDC drive

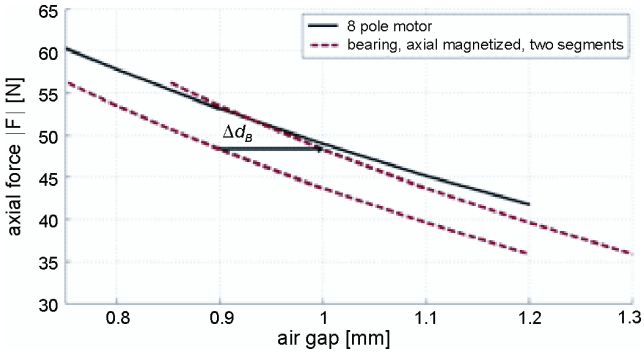

Fig. 10. Comparison of absolute forces

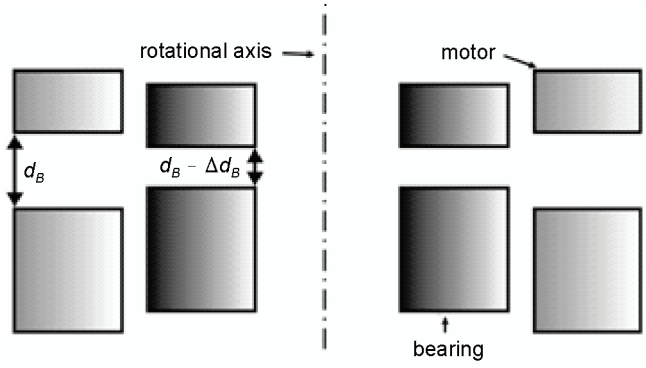

Fig. 11. Assembly of motor and bearing

Therefore the absolute axial forces of the motor and the bearing are nearly identical in the air gap between 0.9 and 1 mm. Possible deviations from the working point can be stabilized by the aforementioned hydrodynamic bearing.

4. Conclusions

Ventricular Assist Devices (VADs) are required to support the weak human hearts of patients, suffering from cardiovascular diseases, to generate a sufficient perfusion of the body. When designing the VAD components, the physical constraints of the human body have to be considered to avoid blood and tissue damage. In order to prevent an overheating of the blood caused by excessive losses and to avoid blood damage by shear forces, passive and contactless bearings are desirable for their drives. For the previous version of the presented drive design only a hydrodynamic bearing was applied to meet this requirement. Due to higher axial forces of the described drive, permanent magnet bearings are investigated and integrated in its design to support the hydrodynamic bearing. It turned out that a double segmented axial magnetized topology generates higher repelling forces and axial stiffness, when compared to a non segmented topology. Nevertheless further modifications of the drive design, such as a reduced number of poles as well as different air gap thicknesses for the motor and the bearing, are required. While the magnetic bearing compensates the major part of the axially attracting forces in the drive, the hydrodynamic stabilizes it in a motor air gap range between 0.9 and 1 mm.

In the near future the design of the hybrid bearing has to be validated by measurements. But before additional aspects such as the radial force and stiffness as well as the resistance against tilt of the bearing have to be studied.

References

[1] World-Health-Organization, Causes of Death 2008 Summary Tables, http://www.who.int/evidence/bod/, Health Statistic amd Informatics Department, Genf, Switzerland (2011).

[2] Copeland J.G., Smith R., Arabia F. et al., *Cardiac replacement with a total artificial heart as a bridge to transplantation.* N. Engl. J. Med. 351: 859-867 (2004).
[3] Thoratec Cooperation, http://www.thoratec.com/, accessed May (2011).
[4] Miura H., Arai S., Kakubari Y. et al., *Improvement of the transcutaneous energy transmission system utilizing ferrite cored coils for artificial hearts*. IEEE J MAG 42(10): 3578-3580 (2006).
[5] Hoshi H., Shinshi T., Takatani S., *Third-generation blood pumps with mechanical noncontact magnetic bearings.* The 13th Congress of the International Society for Rotary Blood Pumps, ISRBP, Tokyo (2011).
[6] Pohlmann A., Lessmann M., Finocchiaro T. et al., *Numerical computation can safe life: FEM simulations for the development of artificial hearts.* The 14th International Conference on Electromagnetic Field Computation, CEFC, Chicago, USA, May (2010).
[7] Samuel Earnshaw, *On the nature of the molecular forces which regulate the constitution of the luminiferous ether.* Transactions of the Cambridge Philosophical Society 7: 97-112 (1842).